International Journal of Mechanical and Production Engineering Research and Development (IJMPERD)
ISSN (P): 2249-6890; ISSN (E): 2249-8001
Vol. 9, Issue 5, Oct 2019, 665-678

CRUDE OIL BASED NANOFLUIDS FLOW ON INCLINED WALL

JAAFAR ABDUL ABBAS ABBOOD AL NASRAWI, ROZAINI BIN ROSLAN & H. BAREM

Faculty of Applied Sciences and Technology,

Universititun Hussein Onn Malaysia, Parit Raja, Batupahat, Johor, Malaysia

ABSTRACT

In this research work, we investigated the MHD inclined wall over a nonlinear prone stretching/shrinking plate surface on a crude oil based nano fluids flow. Most specifically, the effects of various parameters namely; suction, magnetic, heat source, thermal radiative on temperature in the presence of crude oil based SWCNTs. We used transformation of similarity to lessen the partial differential equation (PDE) to ordinary differential equations (ODE) for the nonlinear governing equation along with their related boundary conditions. The result of the lessened ODEs is unfolded and explained numerically with the application of the fourth/fifth system Runge-Kutta Fehlberg-technique together with procedure and practice of shooting- technique, utilizing Maple 18 code. The result obtained indicated that there is significant positive correlation stretching/shrinking in the presence of SWCNTs-crude oil. Sphere shape SWCNTs-crude oil with the different parameters plays significant roles in the temperature distribution with an increase in various nanoparticles. The rate of heat transfers for sphere-shape is more important when compared and balanced it to the shapes of other nanoparticles in the constructed circulating system in the presence of the magnetic field.

KEYWORDS: MHD Nanofluid Flow SWCNTS, Nanofluid, Stretching/Shrinking & Magnetic Field

Received: Feb 28, 2019; **Accepted**: Mar 22, 2019; **Published**: Sept 21, 2019; **Paper Id.**: IJMPERDOCT201958

Original Article

INTRODUCTION

Historically, in 1995, Stephen Choi introduced the term nanofluid (Choi et. al, 1995). Nanofluid is referred to as a liquid which contain dispersion of submicronic solid particles, which is called nanoparticles. The fundamental objective of using nanoparticles is basically to diffuse rigid particles in order for the thermal conductivity to be boosted. The apparent (surface) region to the ration of the volume of nanoparticle is very huge. This however, fetches a huge and enormous propelling pressure for diffusion, most specifically, when the temperature is raised. In real-time application, nanofluid has been investigated to be boosting the transfer of heat more than 50percentespecially when the nanoparticle volume ratio to the base-oil is below 0.3% [1]. When comparing nanofluid with other based fluid, nanofluid has an upper hand on boosting in thermal conductivity [2], [3], [4], [5].

On top of these, many researchers have carried out research activity to improve the thermal conductivity properties so that it would behave the same as fluid but has thermal conductivity as metal by adding and testing conductive solids into fluids, [3], [6], [4], [5], [2]. Nanoparticle used are usually made of metal (Al, Cu), oxides (Al2O3) and SWCNTs just to mention a few. In view of this, and because of the new additive working fluid, it is very important and necessary to research on the impact of heat transfer behaviour and characteristics, namely, thermal conductivity, heat transfer, viscosity and so on. In this research direction, mathematicians, physicists and engineers are among the academic researchers who contribute to the knowledge of thermal conductivity. Though research has shown that nanofluid provides higher transfer of heat with respect of the based fluid [7], [8]. [9] but

regarding the oil-based research direction, it is observed that only a few research are available with respect to the nanofluid thermal particle [10].

In industrial applications, nanoparticles have been used to avoid overheat of the instrument [11]. Thus, nanoparticle plays an important role as the coolant substance to transfer heat. An example of such is our computer system [12]. The heat sink helps to absorb and cool the heat generated in the system, thereby avoiding being overheated. This is because the diameter of the nanoparticles is less than 100nm and this condition will affect the properties of the liquid surface area to enhance the heat transfer compared to the micron-size particle [13]. As far as development in technology and industries remain, the exchange of thermal conductivity must be updated from time to time. The old method of thermal conductivity, which is referred to as traditional means of transferring heat fluid such as Maxwell theories [14]has a lot of difficulties in improving the cooling capacities [15], [16], [17], and is not sufficient or cannot explain behaviour of the thermal conductivity of nanoparticle. However, recently, effort has been carried out to improve and report the thermal conductivity's property by making an addition into the based fluid [18].

Several researchers including [19] used nanofluids to improve heat transfer from different geometries under different thermal boundary conditions. Numerous investigations about heat transfer issue in micro channels and different geometries have been considered by specialists. Presently, with the connection of industries and engineering equipment enhancement, the benefit of the nanoparticle has been promoted. Different research has been investigated and reported on the nanoparticle effects on copper [20], oscillatory enhancement [21], stead and unsteady squeeze flow[14], just to mention a few. The application of this has been utilized in several aspects such as engineering [22], chemical production [23], automotive [24], power formation of a power plant [25], beforehand nuclear systems [26].

Various nanoparticle shapes have been utilized over the experiment [27], [28], which presented the first kind of experimental analysis. The improvement and enhancement of thermal conductivity is as a result of the form and appearance of the included nanoparticle into the suspension. [29]analysed role of the silicon carbide (SiC) nanoparticles where they admitting the shape and appearance affirm disc or platelet, and consistently diffused in the water on mechanical assets and thermal conductivity enrichment.

Study about Magneto-hydrodynamic (MHD) on interaction of conducting fluids with electromagnetic phenomena was studied recently [30]. The MHD flow meter and MHD pump, the run of an electric conducting fluid with the presence of magnetic field is important in order to complete the MHD theorem [3].

A few shapes of the nanoparticles that have been analysed include cylindrical rods [27], and shuttle-like shape [31]. The interpretation of nanofluids inside a paddock was examined[32]. The rigid particle dispersion was analysed, interpreted and reported in the research. A research to investigate and report the reactions of nanoparticles on additive-free convection boundary layer stream move was conducted in[33]. The authors discussed analytically the additive-free convective boundary-layer flow of a nanofluid past a vertical plate. This ideal was recently extended in [34]. This indicated the apparent (surface) region to the ratio of the volume of nanoparticle is very huge.

In this investigation, our aim is to report the effects of various parameters namely; heat generation, chemical reaction, thermophores is, radiative heat flux, Brownian motion, and magnetic on temperature in the presence of kerosene based Carreau SWCNTs.

MATHEMATICAL FORMATION

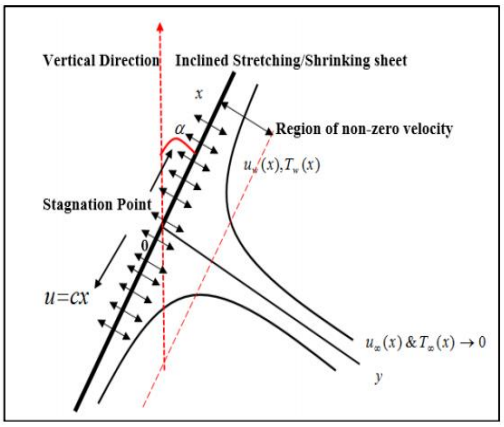

Figure 1: Physical Configuration of Stretching/Shrinking Sheet and Coordinate System – Crude Oil Based.

In this paper, the aim of this work is to clarify several aspects of a mathematical-form to reportinvestigation on the MHD inclined wall over a nonlinear prone stretching/shrinking plate surface on a crude oil based nanofluids flow with extensible depth. $U_w = cx^n$is the velocity used in the paper to construct the stretching sheet, and c represents the constant dimensionless and n is the parameter for nonlinear stretched velocity for the constructed sheet. Based on the construct sheet as displayed in figure 1, the x-axis is controlled and governed through the unbroken and steady stretching/shrinking plate. Also, the axis of our y is generally measured to the axis of x. It is considered that the moving fluid happens at when yϵi, very all i ≻ 0 and the temperature at the prone stretching/shrinking plate happens at a constant measure $T_w \in$ i, all i ≻ 0. Besides, the temperature of the nanofluid's ambient is governed by the constant measure of T_w as y. We have 00, 900 and 00<a<900 as the angles of inclination measured counter clockwise for the vertical, horizontal and overall inclined stretching/shrinking plate, correspondingly. $B(x) = B_0 x^{(m-1)/2}$is theset to be the thickness of sheet,B_0 is set to be its constant dimensionless. The review of the model is constructed to be pleased only for $m \neq 1$, the reason is that of for $m = 1$, the issue lessen the flat-sheet.

Based on the approximation of the boundary layer, equation (1) -(3) give the relevance of the physical governing-equations, continuity, momentum and energy, as obtain below[35]:

$$\frac{\partial u}{\partial x} + \frac{\partial v}{\partial y} \tag{1}$$

$$u\frac{\partial u}{\partial x} + v\frac{\partial v}{\partial y} = \frac{\mu_{nf}}{\rho_{nf}}\frac{\partial^2 u}{\partial y^2} + \frac{(\rho\beta)_{nf}}{\rho_{nf}} g(T - T_\infty)\cos(\alpha) - \frac{\sigma_{nf} B^2(x)}{\rho_{nf}} u \tag{2}$$

$$u\frac{\partial T}{\partial x} + v\frac{\partial T}{\partial y} = \frac{\mu_{nf}}{\rho_{nf}}\frac{\partial^2 T}{\partial y^2} + \frac{1}{(\rho c)_{nf}}\frac{\partial q_r}{\partial x} + \frac{\mu_{nf}}{(\rho c)_{nf}}\left(\frac{\partial u}{\partial y}\right)^2 + \frac{Q_0}{(\rho c)_{nf}}(T_w - T_\infty) \tag{3}$$

Boundary conditions

$$\text{As } y = 0, U_w(x) = \pm cx^n; v = v_w, T = T_w = T_\infty bx^n; \text{ as } y;\ T = T_\infty; u \to 0 \to \infty \tag{4}$$

u and *v* are fix to represent the component of the velocity towards the direction of *x* and *y* axis, respectively, while for the stretching plate, *c* is a constant value constant measure $c \in i$, all $i \succ 0$ and for the shrinking sheet we have that *c*<*o*. *T* represents the temperature of the nanoparticles and the acceleration due to force (gravity) is represents as *g*,

v_w-concentration for the nanofluid near the wall, C_∞- ambient concentration of the nanofluid, T - nanofluid temperature, C - Nano fluid concentration, ρ_{nf} - nanofluid effective density, α_{nf} - nanofluid thermal diffusivity, μ_{nf} - coefficient of nanofluid dynamic viscosity, $(\rho c_p)_{nf}$ - nanofluid heat capacitance.

$$\rho_{nf} = (1-\xi)\rho_f + \xi\rho_s . \mu_{nf} = \frac{\mu_f}{(1-\xi)^{\frac{5}{2}}}, (\rho\beta)_{nf} = (1-\xi)(\rho\beta)_f + \xi(\rho\beta)_s, (\rho c_\rho)_{nf} = (1-\xi), (\rho c_\rho)_f + \xi(\rho c_\rho)_s$$

$$\alpha_{nf} = \frac{k_{nf}}{(\rho\, c_p)_{nf}}, \frac{k_{nf}}{k_f} = \left\{\frac{(k_s + (l-1)k_f) - (l-1)\zeta(k_f - k_s)}{(k_s + (l-1)k_f) + \zeta(k_f - k_s)}\right\}, \sigma_{nf} = (1-\zeta)\sigma_f + \zeta\sigma_s \left(D_B\right)_{nf} = (1-\zeta)\left(D_B\right)_f \quad (5)$$

Maxwell design was cultivated to assign the dynamic thermal or electrical conductivity of liquid-solid suspensions. Let σ_f and σ_s - base fluid and nanoparticle electrical conductivity, $k_{f\ and\ k_s}$base-fluid, nanoparticle thermal conductivity, ζ - volume fraction of nanoparticle, ρ_f and ρ_s - base fluid and nanoparticle density, $\sigma_{f\ and\ \sigma_s}$- based fluid, and nanoparticle electrical conductivity, μ_f - dynamic viscosity for the base fluid, k_{nf} - nanofluid effective thermal conductivity. Rosseland's dissipation for the radiative heat flux, $q_r = -\frac{4\sigma^*\partial T^4}{3k^*\partial y}$ [36], k^* - Rosseland signify absorption coefficient. σ^* - Stephen-Boltzmann constant, the regime T^4 is defined as a result of the radiation in linear function for the temperature and T^4 is addressed by Taylor's series around T_∞ as $T^4 = 4T_\infty^3 T - 3T_\infty^4$.

The executing similarity conversions with the fulfilment of the analysis is analysied below:

$$\psi = \left[\frac{2\nu_f U_0 (x+b)^{(m-1)}}{m+1}\right]^{\frac{1}{2}} f(\eta), \eta = \left[\frac{(m+1)U_0 (x+b)^{(m-1)}}{2\nu_f}\right]^{\frac{1}{2}} y, \theta(\eta) = \frac{T - T_\infty}{T_w - T_\infty}, \phi(\eta) = \frac{C - C_\infty}{C_w - C_\infty}, \quad (6)$$

ν_f - the fluid kinematic viscosity and ψ - represents the function of the stream, constructed as$u = \frac{\partial\psi}{\partial y}, v = \frac{\partial\psi}{\partial x}$, which adequately attends the Equation (1)- (3) are transformed to the dimensionless form as follow

$$f^{III} + (1-\emptyset)^{2.5}\left\{\left((1-\emptyset) + \emptyset\frac{\rho_s}{\rho_f}\right)\left(ff^{II} - \frac{2m}{m+1}(f^I)^2\right)Mf^I + \frac{2m}{m+1}(1-\emptyset) + \emptyset\frac{(\rho\beta)_s}{(\rho\beta)_f}(Ri\cos(\alpha)\theta\right\} \quad (7)$$

$$\frac{1}{Pr_{eff}}\theta^{II} + ((1-\emptyset)\emptyset\frac{(\rho c_p)_s}{(\rho c_p)_f})(\left(\frac{2m+1}{m+1}\right)f\theta^I - \left(\frac{4m}{m+1}\right)f^I\theta + \frac{E_c}{(1-\emptyset)^{2.5}}(f^{II})^2 + \frac{1}{m+1}\frac{Q}{Pr}\theta = 0 \quad (8)$$

$$\phi'' + (A1).\left(\frac{1}{(A1)}\frac{Nt}{Nb}\theta'' + LeF\theta' - Le\gamma\phi\right) = 0 \quad (9)$$

With boundary conditions are:

$$\text{At } \eta = 0: f = s, f^I = \pm 1, \theta = 1; at\ \eta \longrightarrow \infty, \theta \to 0 \quad (10)$$

$$K_{nf} = (k_s + (e-1)(k_f) - (e-1)\zeta(k_f - (k_s), K_f = (k_s + (e-1)(k_f) - \zeta(k_f - (k_s), B = \left(1 - \zeta + \zeta\frac{\rho_s}{\rho_f}\right), T = \frac{K_{nf}}{K_f}, \quad (11)$$

$$E=\left(1-\zeta+\zeta\frac{\rho_s(cp)_s}{\rho_f(cp)_f}\right),\ A=\left(1+\frac{3\left(\frac{\sigma_s}{\sigma_f}-1\right)\zeta}{\left(\frac{\sigma_s}{\sigma_f}+2\right)-\left(\frac{\sigma_s}{\sigma_f}-1\right)\zeta}\right),G=(1-\zeta)^{2.5},\ A1=\frac{1}{1-\zeta} \tag{12}$$

Here $\alpha=B\sqrt{\frac{U_0(m+1)}{2\nu_f}}$ - depth parameter of the corresponding wall and $\eta=B\sqrt{\frac{U_0(m+1)}{2\nu_f}}$ - dependent plate of the surface. So, if we substitute the transformations, $f(\alpha)=f(\eta-\alpha)=f(\eta),\ \theta(\alpha)=\theta(\eta-\alpha)=\theta(\eta)$, and $\phi(\alpha)=\phi(\eta-\alpha)=\phi(\eta),$ the above equations takes the form

$$f^I(\eta)=p;\ p^I(\eta)=q,\theta^I(\eta)=t \tag{13}$$

$$f^I(\eta)=(1-\emptyset)^{2.5}\left\{\left((1-\emptyset)+\emptyset\frac{\rho_s}{\rho_f}\right)\left(\frac{2m}{m+1}p^2-fq\right)+Mp-\frac{2m}{m+1}(1-\emptyset)+\emptyset\frac{(\rho\beta)_s}{(\rho\beta)_f}(Ri\cos(\alpha)\theta\right\}t^I(\eta)=$$

$$Pr_{eff}[\left((1-\emptyset)\emptyset\frac{(\rho c_p)_s}{(\rho c_p)_f}\right)\left(\frac{4m}{m+1}\right)p\theta-\left(\frac{2m+1}{m+1}\right)ft-\left(\frac{E_c}{(1-\emptyset)^{2.5}}\right)q^2-(\frac{1}{m+1}\frac{Q}{Pr})\theta \tag{14}$$

with boundary's conditions are

$$f(\alpha)=\alpha\frac{1-m}{1+m},\ f'(\alpha)=1,\theta(\alpha)=1,\phi(\alpha)=1;\ f'(\infty)=0,\theta(\infty)=0,\phi(\infty)=0 \tag{15}$$

$M=\frac{2\sigma_f B_0^2}{U_0(m+1)(x+b)^{m-1}\rho_f}$ - the magnetic parameter, $W=(m+1)\frac{U_0^3(x+b)^{3m-1}}{2\nu_f}\Gamma^2$ - the Weissenberg number, $\Pr_f=\frac{\Pr}{\left(\frac{k_{nf}}{k_f}+\frac{4}{3}R\right)}$ - the effective Prandtl number, where $\Pr=\frac{(\mu c_p)_f}{k_f}$ is the Prandtl-number, $\gamma=\frac{2K}{U_0(m+1)(x+b)^{m-1}}$ - parameter of the chemical reaction, $\mathrm{Re}_x=\frac{xU_0(x)}{\nu_f}$ - number of the local Reynolds, $E_1=\frac{E_0}{B_0U_0(x+b)^m}$ - parameter of the electric, $N_b=\frac{(\rho c)_s(D_B)_f(C_w-C_\infty)}{(\rho c)_f\nu_f}$ - parameter for the Brownian motion, $N_t=\frac{(\rho c)_s(D_T)_f(T_w-T_\infty)}{(\rho c)_f\nu_f T_\infty}$ - parameter of the thermophoresis, $Le=\frac{\nu_f}{(D_B)_f}$ - number of the Lewis and $R=-\frac{4\sigma^* T_\infty^3}{k_f k^*}$ - the solar radiation-conduction parameter. Besides, the physical resources of engineering hits of materials boosting application with the local coefficient of the friction-skin, C_f, Nusselt-number Nu_x Sherwood-number Sh_x can be obtained below

$$\mathrm{Re}_x^{\frac{1}{2}}C_f=\frac{1}{(1-\zeta)^{2.5}}\left(\frac{m+1}{2}\right)^{\frac{1}{2}}f''(0),\ \mathrm{Re}_x^{-\frac{1}{2}}Nu_x=-\left(\frac{k_{nf}}{k_f}+\frac{4}{3}R\right)\left(\frac{m+1}{2}\right)^{\frac{1}{2}}\theta'(0),\ Sh_x\,\mathrm{Re}_x^{-\frac{1}{2}}=-\frac{1}{(1-\zeta)}\left(\frac{m+1}{2}\right)^{\frac{1}{2}}\phi'(0) \tag{16}$$

RESULTS AND DISCUSSIONS

Here, shooting method is used to solve equation along with the boundary condition in equation. This method has been investigated by many researchers [37], [9]. The simulation is computed for the various parameters effects on temperature,$-\theta'(0)$. We omitted the solution method in order for us to conserve space. However, in order to validate our method, Radiative heat for [38] with present article confirmed the present article with previous article. We compared the chemical reaction in articles which validate for this parameter and the profile as shown in Figure 8. Table 2 displayed the data Magnetic field deposition for the two stretching and shrinking plate case with the thermal magnetic. It is observed from the stretching sheet that for the case of sphere nanoparticle shape, that M is increasing with the reduction in stretching sheet, which indicated that the moving flow is decelerated. This reaction happened for all the three nanoparticle investigated in this paper, but it is interesting and fascinating and to note that sphere has the upper heat transfer when compare to the other counterparts. This is also applicable between boundary layer at when $M = 0.5, M = 1.0$ and $M = 3.0$ the temperature is increased with the increase in the thermal magnetic. Also for the aspect of shrinking sheet, it indicated that for sphere at when $M = 0.5, M = 1.0$ and $M = 3.0$, when magnetic field is increasing. This show that heat transfer maintain the same effect between when $M = 0.5, M = 1.0$ and $M = 3.0$ for sphere shape. For the cylinder and lamina shapes, the result obtained indicated a fluctuating reaction. It increases when M = 0.6 and later dropped when M = 1.0 before it went up again while the sphere maintained a constant flow reaction. The only difference is that the rate of increase of the sphere for the temperature,$(\theta(\eta))$is higher when compare with the cylinder and laminar shapes, which show that the sphere shape is more relevance when compared to the other two shapes in the flow system. For the case of cylinder, the result indicates that when magnetic field is increasing, the temperature, $(\theta(\eta))$ is fluctuating with thermal magnetic. It is quite obvious to know and conclude that the rate of heat transfers for sphere-shape is more important when compared to the shapes of other nanoparticles in the constructed flow system in the presence of the magnetic field.

Table 1: Thermo-Physical Resources for the Fluid with the Nanoparticles

	$\rho(kg/m^3)$	$c_p(J/kgK)$	$k(W/mK)$	$\sigma(\Omega^{-1}m^{-1})$
Crude oil	884	1910	0.144	4.02
SWCNTs-kerosene	2600	42.5	6600	1.26

Nanoparticle Shapes

Sphere ($M = 3.0$)

Cylinder ($M = 6.3628$)

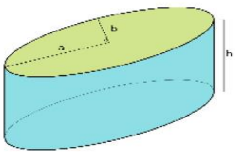

Lamina ($M = 16.1576$)

Figure 1: Nanoparticles Shapes.

Table 2: Heat Transfer Rate for Different Values of *M*

M	**Stretching $-\theta'(0)$**	**Shrinking $-\theta'(0)$**	**Remark**
0.5	834.1423599	-5.8430883709	Sphere
1.0	829.1301476	-6005.6769526	
3.0	809.3543868	-983.41351382	
0.5	796.9743233	145.43504733	Cylinder
1.0	793.0668241	-7238.3479274	
3.0	777.6632851	-843.82974878	
0.5	832.7584593	18.2627425948	Lamina
1.0	827.7545899	-5995.8876344	
3.0	808.0117459	-981.83523721	

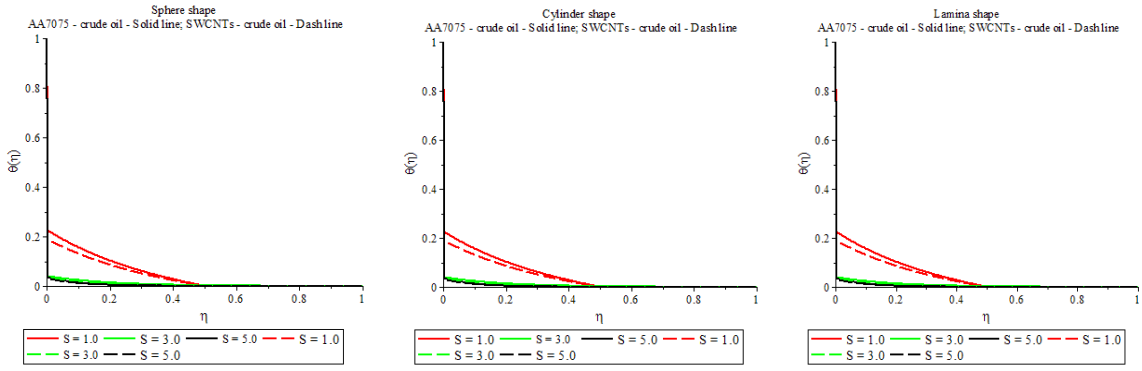

Figure 2: Suction Effects (Shrinking) on Temperature Profiles.

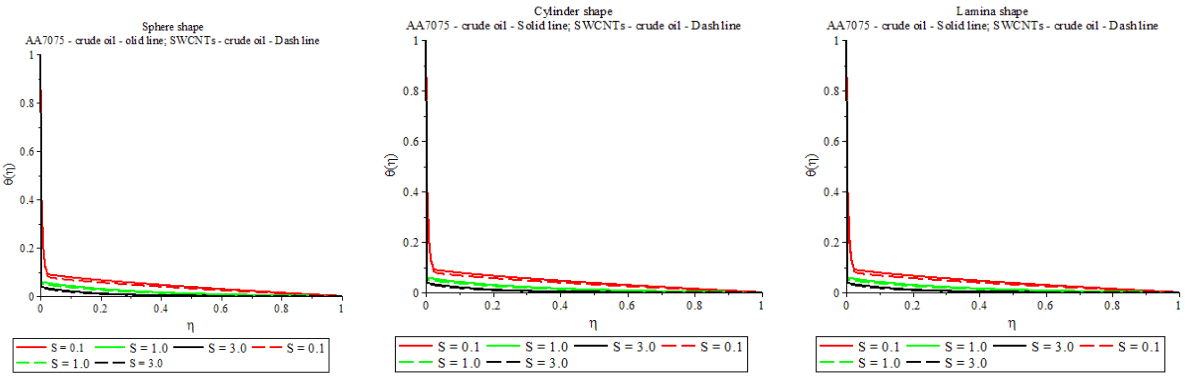

Figure 3: Suction Effects (Stretching) on Temperature Profiles.

Figure 2 and 3, discussion of suction parameter, S

The suction reactions temperature's $(\theta(\eta))$ effect profiles for the two shrinking and stretching is hereby displayed in figure (2) – (3). The displacements show with different nanoparticle shapes, sphere, cylinder and lamina. It shows in the figures that temperature, $(\theta(\eta))$circulation for all nanofluids increase and equivalently the rate of transfer in the heat concentration increase with expansion and enlargement in suction parameter, S. The profile indicated that shrinking shows an excellent performance than the stretching. Particularly, between boundary layer at when, $S = 1.0, S = 3.0$ and, $S = 5.0$. The boundary of the thermal surface depth of sphere – crude oil is dominant than the its counterparts nanofluids shapes. It displays from the profile that the rate of heat transfers for SWCNTs – crude oil is more noteworthy and remarkable as balanced to its counter parts nanofluids in the circulation stream system. The effect of thermal radiation is such that, $S = 1.0, S = 3.0$ and, $S = 5.0$ the temperature is increasing with increase the of suction parameter, S.

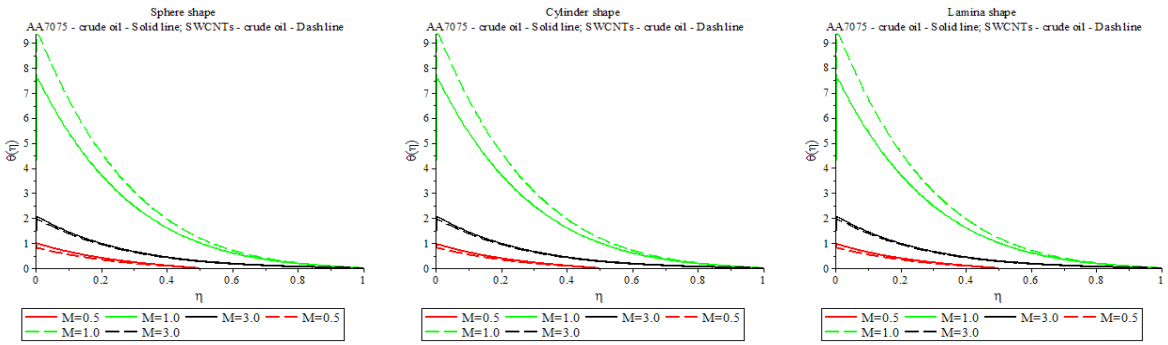

Figure 4: Magnetic Effects (Shrinking) on Temperature Profiles.

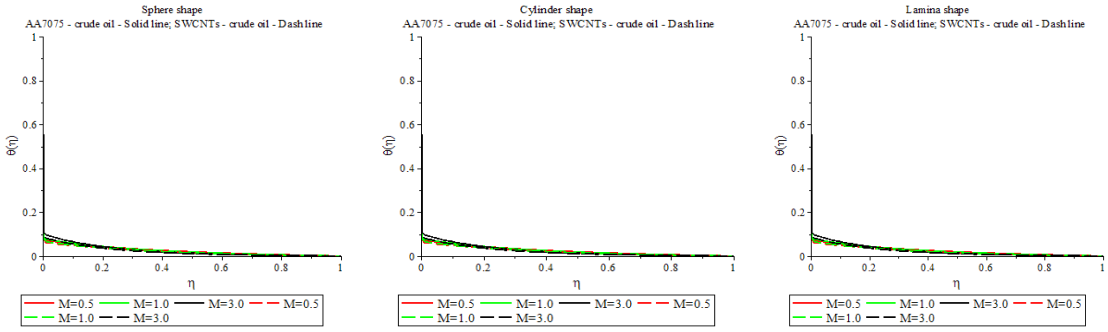

Figure 5: Magnetic Effects (Stretching) on Temperature Profiles.

Figure 4 and 5, discussion of thermal magnetic parameter, *M*

The thermal magnetic parameter, Mreactions temperature's effect profiles for both shrinking and stretching is hereby displayed in figure. (4) – (5). The increase in thermal magnetic parameter, R resulted in the increase in the temperature of the thermal magnetic depth of the boundary layer. The displacements show with different nanoparticle shapes, that is, sphere, cylinder and laminar. It shows in the figure that temperature, $(\theta(\eta))$ circulation for all nanofluids increase and equivalently the mbgghrate of transfer in the heat concentration increase with expansion and enlargement in thermal magnetic power. Particularly, between boundary layer at when $M = 0.5, M = 1.0$ and $M = 3.0$ boundary of the thermal surface depth of sphere – crude oil is dominant than the its counterparts nanofluids. It displays from the profile that the rate of heat transfers for SWCNTs – crude oil is more noteworthy and remarkable as balanced to its counterparts nanofluids in the circulation stream system. The effect of thermal radiation is such that $M = 0.5, M = 1.0$ and $M = 3.0$ the temperature increasing with the increase in thermal magnetic parameter, M. The profile indicated that shrinking shows an excellent performance than the stretching.

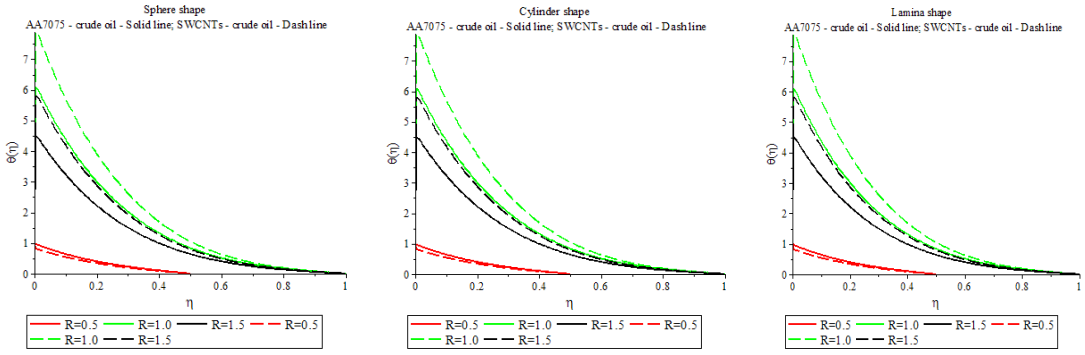

Figure 6: Thermal Radiation Effects (Shrinking) on Temperature Profiles.

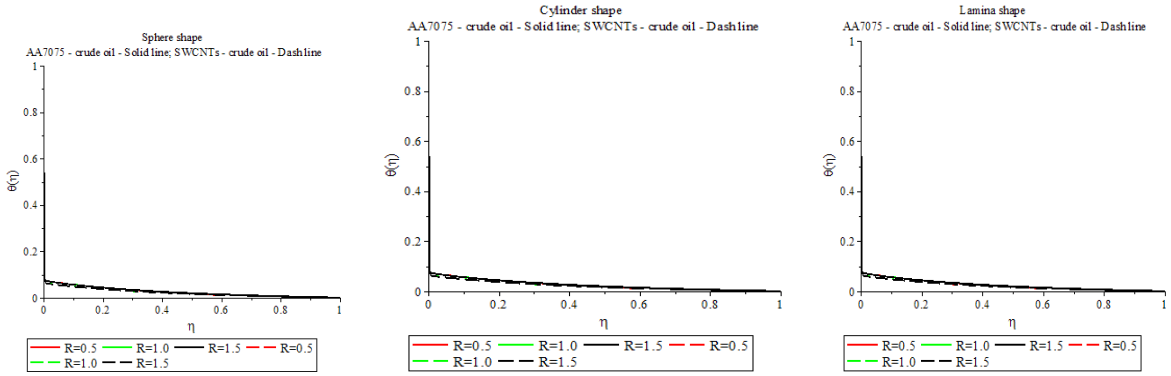

Figure 7: Thermal Radiation Effects (Stretching) on Temperature Profiles.

Figure 6 and 7, discussion of thermal radiation parameter, R

The radiation parameter, R reactions temperature's effect profiles for both shrinking and stretching is hereby displayed in figure (4) – (5). The profile indicated that shrinking shows an excellent performance than the stretching. The displacements show with different nanoparticle shapes (sphere, cylinder and laminar). The thermal radiation for the shrinking show a significant reaction in boosting the temperature. The increase in thermal radiation parameter, R resulted into increase and boosting in the temperature of the thermal surface depth of the boundary layer. It shows in the figure that temperature, $(\theta(\eta))$ circulation for all nanofluids decrease but in contrast the rate of transfer in the heat concentration increase with expansion and enlargement in thermal radiation strength. Particularly, between boundary layer at when $R = 0.5, R = 1.0$ and R =1.5. The boundary of the thermal surface depth of sphere– crude oil is dominant than its counterparts nanofluids. It displays from the profile that the rate of heat transfers for SWCNTs – crude oil is more noteworthy and remarkable as balanced to its counterparts nanofluids in the circulation stream system. The effect of thermal radiation is such that $R = 1., R = 3$ and $R = 3.0$ for the temperature increase with increase in the thermal radiation in the same trend with thermal radiation parameter, R the temperature is increasing and the deference between low and high electric are slightly decreased. For the lamina shape, the result obtained also mentioned same result over the sphere and cylindrical shapes.

Figure 8 and 9, discussion of heat source parameter, q

The magnetic reactions temperature's effect profiles for both shrinking and stretching is hereby displayed in figure (8) – (9). The profile indicated that shrinking shows an excellent performance than the stretching. The displacements show with different nanoparticle shapes (sphere, cylinder and laminar). The thermal radiation for the shrinking shows a significant reaction in boosting the temperature.

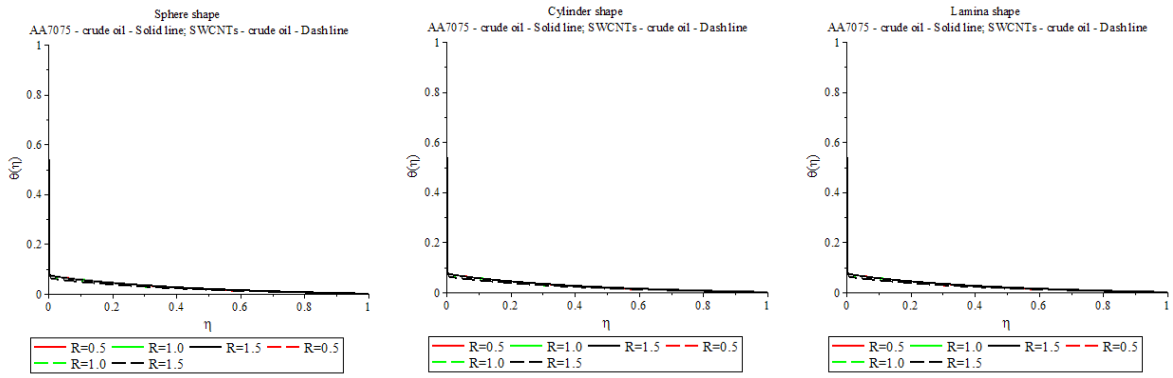

Figure 8: Heat Source Effects (stretching) on Temperature Profiles.

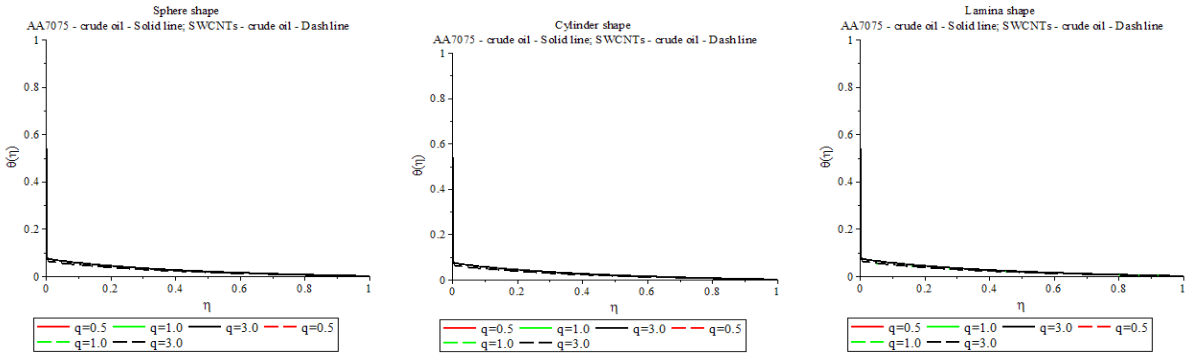

Figure 9: Heat Source Effects (Stretching) on Temperature Profiles.

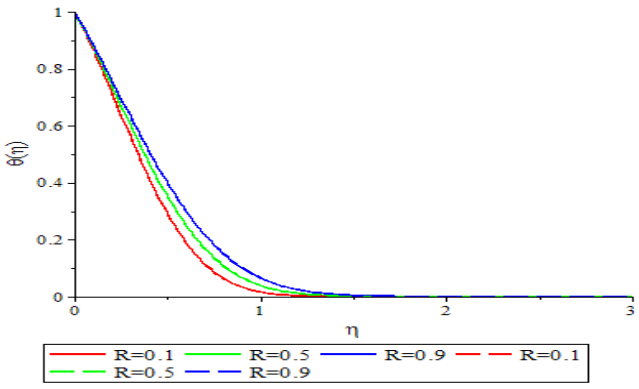

Figure 10: Compare the Radiative Heat for [38] with Present Article.

The increase in heat source parameter, $q$resulted in increase in the temperature of the thermal surface depth of the boundary layer. It shows in the figure that temperature, $(\theta(\eta))$ circulation for all nanofluids increase and equivalently the rate of transfer in the heat concentration increase with expansion and enlargement in heat source parameter, δ. Particularly, between boundary layer at when, $q = 0.5, q = 1.0$ and $q = 0.5$. boundary of the thermal surface depth of sphere – crude oil is dominant than the its counterparts nanofluids. It displays from the profile that the rate of heat transfers for SWCNTs – crude oil is more noteworthy and remarkable as balanced to its counterparts nanofluids in the circulation stream system. The effect of thermal radiation is such that, $q = 0.5, q = 1.0$and, $q = 0.5$ the temperature is increasing with increase the heat source parameter, q

To confirm the present article with previous article, we compare the chemical reaction in articles which is validate for this parameter. The result with the theoretical solution for the velocity profile is observed to be very good.

CONCLUSIONS

The effects of various parameter namely; suction parameter, S, of thermal magnetic parameter, M, thermal radiation parameter, R, heat source parameter, $q$on temperature, $(\theta(\eta))$are investigated in this paper. Graphically, the results are presented and the conclusion is drawn on the various effect on the temperature, $(\theta(\eta))$.

The boundary conditions of the ODE were satisfied and solved using the same value of the governing parameter. We took several variable of the parameter as manipulated and other parameters as the constant variable, we were able to get a lot of results and reaction, which include;

- Sphere shape SWCNTs-crude oilwith the different parameters plays significant roles in the temperature distribution with an increase in various nanoparticles.
- For the cylinder and lamina shapes, the result obtained indicated a fluctuating reaction. It increases when M = 0.6 and later dropped when M = 1.0 before it went up again while the sphere maintained a constant flow reaction. In the capacity of magnetic on the profile, the velocity decrease when the parameter M is increase. From the profile boundary layer thickness, is indicated that the thermal radiation, heat generation and chemical is large which shows that the parameter has high effect on temperature.
- shrinking shows an excellent performance than the stretching. Most specifically it plays significant roles in the temperature distribution with an increase in various nanoparticles.

- The profile indicated that shrinking shows an excellent performance than the stretching. The increase in thermal radiation parameter, R resulted into increase and boost in the temperature, $(\theta(\eta))$ of the thermal surface depth of the boundary layer.
- It is quite obvious and clear to know that the rate of heat transfers for sphere-shape is more important when compared to the other shapes of nanoparticle in the flow system.
- It shows in the figure that temperature, $(\theta(\eta))$ circulation for all nanofluids decrease but in contrast the rate of transfer in the heat concentration increase with expansion and enlargement in thermal radiation strength

ACKNOWLEDGMENTS

The authors would like to acknowledge the financial support received from the UniversitiTun Hussein Onn Malaysia, Grant TIER1/H072.

REFERENCES

1. *Y. J. Hwang Et Al., "Investigation On Characteristics Of Thermal Conductivity Enhancement of Nanofluids," Curr. Appl. Phys., Vol. 6, No. 6 Spec. Iss., Pp. 1068–1071, 2006.*
2. *R. Kandasamy, R. Dharmalingam, And K. K. S. Prabhu, "Thermal And Solutal Stratification on Mhd Nanofluid Flow Over a Porous Vertical Plate," Alexandria Eng. J., Vol. 57, No. 1, Pp. 121–130, 2018.*
3. *E. Kabeel, E. M. S. El-Said, And S. A. Dafea, "A Review of Magnetic Field Effects on Flow And Heat Transfer In Liquids: Present Status And Future Potential For Studies And Applications," Renew. Sustain. Energy Rev., Vol. 45, Pp. 830–837, 2015.*
4. *P. Singh And M. Kumar, "Mass Transfer In Mhd Flow of Alumina Water Nanofluid Over A Flat Plate Under Slip Conditions," Alexandria Eng. J., Vol. 54, No. 3, Pp. 383–387, 2015.*
5. *P. Sudarsana Reddy, A. J. Chamkha, And A. Al-Mudhaf, "Mhd Heat And Mass Transfer Flow of A Nanofluid Over An Inclined Vertical Porous Plate With Radiation And Heat Generation/Absorption," Adv. Powder Technol., Vol. 28, No. 3, Pp. 1008–1017, 2017.*
6. *N. Sandeep, C. Sulochana, And B. Rushi Kumar, "Unsteady Mhd Radiative Flow And Heat Transfer of A Dusty Nanofluid Over An Exponentially Stretching Surface," Eng. Sci. Technol. An Int. J., Vol. 19, No. 1, Pp. 227–240, 2016.*
7. *M. Hemmat, W. Yan, M. Akbari, A. Karimipour, And M. Hassani, "Experimental Study On Thermal Conductivity of Dwcnt-Zno / Water-Eg Nano Fl Uids ☆," Int. Commun. Heat Mass Transf., Vol. 68, Pp. 248–251, 2015.*
8. *J. Raza, A. M. Rohni, And Z. Omar, "Mhd Flow And Heat Transfer of Cu–Water Nanofluid In A Semi Porous Channel With Stretching Walls," International Journal Of Heat And Mass Transfer, Vol. 103. Pp. 336–340, 2016.*
9. *R. Kandasamy, R. Mohammad, N. A. B. M. Zailani, And N. F. B. Jaafar, "Nanoparticle Shapes On Squeezed Mhd Nanofluid Flow Over A Porous Sensor Surface," J. Mol. Liq., Vol. 233, Pp. 156–165, 2017.*
10. *S. E. B. Maïga, C. T. Nguyen, N. Galanis, G. Roy, T. Maré, And M. Coqueux, "Heat Transfer Enhancement In Turbulent Tube Flow Using Al2o3 Nanoparticle Suspension," Int. J. Numer. Methods Heat Fluid Flow, Vol. 16, No. 3, Pp. 275–292, 2006.*
11. *K. V. Wong And O. De Leon, "Applications of Nanofluids: Current And Future," Advances In Mechanical Engineering, Vol. 2010. 2010.*
12. *M. R. Islam, B. Shabani, And G. Rosengarten, "Electrical And Thermal Conductivities Of 50/50 Water-Ethylene Glycol Based Tio2 Nanofluids To Be Used As Coolants In Pem Fuel Cells," In Energy Procedia, 2017, Vol. 110, Pp. 101–108.*

13. W. Anderson, D. Kozak, V. A. Coleman, Å. K. Jämting, And M. Trau, "A Comparative Study of Submicron Particle Sizing Platforms: Accuracy, Precision And Resolution Analysis of Polydisperse Particle Size Distributions," J. Colloid Interface Sci., 2013.

14. M. Sheikholeslami, D. D. Ganji, And M. M. Rashidi, "Magnetic Field Effect on Unsteady Nanofluid Flow And Heat Transfer Using Buongiorno Model," J. Magn. Magn. Mater., 2016.

15. M. Hatami, M. Jafaryar, J. Zhou, And D. Jing, "Investigation Of Engines Radiator Heat Recovery Using Different Shapes of Nanoparticles In H<Inf>2</Inf>O/(Ch<Inf>2</Inf>Oh)<Inf>2</Inf>Based Nanofluids," Int. J. Hydrogen Energy, Vol. 42, No. 16, 2017.

16. O. Torsater, B. Engeset, L. Hendraningrat, And S. Suwarno, "Improved Oil Recovery By Nanofluids Flooding: An Experimental Study," In Spe Kuwait International Petroleum Conference And Exhibition, 2012.

17. L. Levidow, D. Zaccaria, R. Maia, E. Vivas, M. Todorovic, And A. Scardigno, "Improving Water-Efficient Irrigation: Prospects And Difficulties of Innovative Practices," Agric. Water Manag., 2014.

18. W. Yu, D. M. France, J. L. Routbort, And S. U. S. Choi, "Review And Comparison Of Nanofluid Thermal Conductivity And Heat Transfer Enhancements," Heat Transf. Eng., Vol. 29, No. 5, Pp. 432–460, 2008.

19. M. Narayana And P. Sibanda, "Laminar Flow of A Nanoliquid Film Over An Unsteady Stretching Sheet," Int. J. Heat Mass Transf., Vol. 55, No. 25–26, Pp. 7552–7560, 2012.

20. J. S. Kim, A. Adamcakova-Dodd, P. T. O'shaughnessy, V. H. Grassian, And P. S. Thorne, "Effects Of Copper Nanoparticle Exposure On Host Defense In A Murine Pulmonary Infection Model," Part. Fibre Toxicol., 2011.

21. K. J. Zwick, P. S. Ayyaswamy, And I. M. Cohen, "16. Oscillatory Enhancement of The Squeezing Flow of Yield Stress Fluids: A Novel Experimental Result," J. Fluid Mech., Vol. 339, Pp. 77–87, 1997.

22. R. J. Macfarlane, B. Lee, M. R. Jones, N. Harris, G. C. Schatz, And C. A. Mirkin, "Nanoparticle Superlattice Engineering With Dna," Science (80-.)., 2011.

23. D. R. Baer, D. J. Gaspar, P. Nachimuthu, S. D. Techane, And D. G. Castner, "Application of Surface Chemical Analysis Tools For Characterization Of Nanoparticles," Analytical And Bioanalytical Chemistry. 2010.

24. S. L. Pal, U. Jana, P. K. Manna, G. P. Mohanta, And R. Manavalan, "Nanoparticle: An Overview of Preparation And Characterization," J. Appl. Pharm. Sci., 2011.

25. Mazumdar, A. J. A. N. I. T. A., & Deka, M. A. N. A. B. (2013). Isolation Of Free Living Nitrogen Fixing Bacteria From Crude Oil Contaminated Soil. International Journal Of Bio-Technology And Research, 3(4), 61–68.

26. Y. Lu, S. K. Das, S. S. Moganty, And L. A. Archer, "Ionic Liquid-Nanoparticle Hybrid Electrolytes And Their Application In Secondary Lithium-Metal Batteries," Adv. Mater., 2012.

27. F. Wibisono, Y. Addad, And J. I. Lee, "A Cfd Assessment For Mixed Convection of Nanofluids For Nuclear Application," In International Conference On Nuclear Engineering, Proceedings, Icone, 2015, Vol. 2015–Janua.

28. H. Xie, J. Wang, T. Xi, And Y. Liu, "Thermal Conductivity of Suspensions Containing Nanosized Sic Particles," Int. J. Thermophys., Vol. 23, No. 2, Pp. 571–580, 2002.

29. S. M. S. Murshed, K. C. Leong, And C. Yang, "Enhanced Thermal Conductivity of Tio2- Water Based Nanofluids," Int. J. Therm. Sci., Vol. 44, No. 4, Pp. 367–373, 2005.

30. Veeresh, C., Varma, S. V. K., & Praveena, D. (2015). Heat And Mass Transfer In Mhd Free Convection Chemically Reactive And Radiative Flow In A Moving Inclined Porous Plate With Temperature Dependent Heat Source And Joule Heating.

International Journal Of Management, Information Technology And Engineering, 3(11), 63–74.

31. *D. Singh Et Al., "An Investigation Of Silicon Carbide-Water Nanofluid For Heat Transfer Applications," J. Appl. Phys., Vol. 105, No. 6, 2009.*
32. *Q. Dong, J. Zhang, Q. Liu, And Y. Yin, "Magnetohydrodynamic Calculation For Electromagnetic Stirring Coupling Fluid Flow And Solidification In Continuously Cast Billets," Steel Res. Int., 2017.*
33. *H. T. Zhu, C. Y. Zhang, Y. M. Tang, And J. X. Wang, "Novel Synthesis And Thermal Conductivity of Cuo Nanofluid," J. Phys. Chem. C, Vol. 111, No. 4, Pp. 1646–1650, 2007.*
34. *K. Khanafer, K. Vafai, And M. Lightstone, "Buoyancy-Driven Heat Transfer Enhancement In A Two-Dimensional Enclosure Utilizing Nanofluids," Int. J. Heat Mass Transf., Vol. 46, No. 19, Pp. 3639–3653, 2003.*
35. *D. A. Nield And A. V. Kuznetsov, "The Cheng-Minkowycz Problem For Natural Convective Boundary-Layer Flow In A Porous Medium Saturated By A Nanofluid," Int. J. Heat Mass Transf., Vol. 52, No. 25–26, Pp. 5792–5795, 2009.*
36. *W. A. A. Khan And I. Pop, "Boundary-Layer Flow Of A Nanofluid Past A Stretching Sheet," Int. J. Heat Mass Transf., Vol. 53, No. 11–12, Pp. 2477–2483, 2010.*
37. *Rashid, F., Dawood, K., & Hashim, A. H. M. E. D. (2014). Maximizing Of Solar Absorption By (Tio2-Water) Nanofluid With Glass Mixture. International Journal of Research In Engineering & Technology, 2, 87–90.*
38. *T. Thumma, O. Anwar Bég, And A. Kadir, "Numerical Study Of Heat Source/Sink Effects On Dissipative Magnetic Nanofluid Flow From A Non-Linear Inclined Stretching/Shrinking Sheet," J. Mol. Liq., 2017.*
39. *E. Magyari And A. Pantokratoras, "Note On The Effect of Thermal Radiation In The Linearized Rosseland Approximation On The Heat Transfer Characteristics of Various Boundary Layer Flows," Int. Commun. Heat Mass Transf., Vol. 38, No. 5, Pp. 554–556, 2011.*
40. *R. Kandasamy, N. A. Bt Adnan, And R. Mohammad, "Nanoparticle Shape Effects On Squeezed Mhd Flow of Water Based Cu, Al2o3 And Swcnts Over A Porous Sensor Surface," Alexandria Eng. J., 2016.*
41. *M. Khan, M. Y. Malik, And T. Salahuddin, "Heat Generation And Solar Radiation Effects On Carreau Nanofluid Over A Stretching Sheet With Variable Thickness: Using Coefficients Improved By Cash And Carp," Results Phys., 2017.*
42. *Qashqaei, A., & Asl, R. G. (2015). Numerical Modeling And Simulation of Copper Oxide Nanofluids Used In Compact Heat Exchangers. International Journal Of Mechanical Engineering, 4 (2), 1, 8.*